Unsteady Aerodynamics of Stationary Elliptic Cylinders in Subcritical Flow

V. J. MODI* AND E. WILAND†
The University of British Columbia, Vancouver, Canada

The aerodynamics of a set of two-dimensional elliptic cylinders with eccentricity of 0.8 and 0.6 is studied experimentally during the organized wake condition. The dynamic calibration of the transducer used for measurement of fluctuating pressures is described in detail. The data on Strouhal number, unsteady pressures and wake geometry are presented as a function of angle of attack during static condition of the models. The effect of Reynolds number on the fluctuating pressure is also examined. The results indicate dependence of the unsteady forces on Reynolds number at zero angle of attack. Basing the Strouhal number on projected width appears to reduce its dependence on the angle of attack of the models. The existence of a large phase angle between the fluctuating pressures is of interest. The wake geometry study indicates a gradual reduction in the ratio of the lateral to the longitudinal spacing with increase in angle of attack.

Nomenclature

C_l = lift coefficient, lift$/(\frac{1}{2})\rho V_\infty{}^2\, 2ac$
$C_{l'}$ = fluctuating lift coefficient (average amplitude)
C_p = pressure coefficient, $(p - p_\infty)/(\frac{1}{2})\rho V_\infty{}^2$
$C_{\bar{p}'}$ = fluctuating pressure coefficient, $\bar{p}'/(\frac{1}{2})\rho V_\infty{}^2$
L = longitudinal spacing between vortices
N_r = Reynolds number, $V_\infty 2a/\nu$
N_s = Strouhal number, fh/V_∞ or $f2b/V_\infty$
S = percentage circumference, measured clockwise from tap 0
V_∞ = freestream velocity
W = lateral spacing between vortices
a = semimajor axis of model
b = semiminor axis of model
c = length of model
d_i = inside diameter of the tube
e = eccentricity, $[1 - (b^2/a^2)]^{1/2}$
f = frequency of vortex formation, Strouhal frequency
h = projected height of model, $2[a^2 \sin^2\alpha + b^2 \cos^2\alpha]^{1/2}$
l = length of the tube
$\bar{l}$ = distance downstream from center of model
p = mean static pressure
p' = fluctuating pressure
$\bar{p}'$ = fluctuating pressure (average amplitude) about mean
p_∞ = freestream mean static pressure
w = tranverse distance from center of model
α = angle of attack
ρ = air density
ν = air kinematic viscosity

Subscripts

max = maximum value of the parameter
rel = relative value

1 Introduction

It is well known that under certain conditions elastically mounted bluff bodies, when exposed to a fluid stream, may exhibit self-induced oscillations. The vibration of smoke stacks, transmission lines, periscopes, aircraft wings, bridges, launch vehicles, etc. has been of interest to engineers. In general, the nature of the forcing function, wake geometry, and Strouhal number form three important parameters in an aeroelastic instability study. The determination of the corresponding information for a set of stationary elliptic cylinders, of eccentricities 0.6 and 0.8, in the Reynolds number range of $3 \times 10^4 - 10^5$ forms the subject of this study.

Strouhal[1] was the first to correlate the periodic vortex shedding with the diameter of a circular cylinder and fluid velocity. This was followed by the classical study of wake geometry and stability by Von Kármán.[2] Ever since, academic and practical interest in the vortex shedding phenomenon has resulted in many theoretical and experimental investigations, e.g., by Roshko, Kovasnay, Tritton, Birkhoff, Humphreys, Schaeffer, Eskinazi, and others. Marris[3] has presented an excellent review of this literature. More recently, Grove et al.[4] as well as Bishop and Hassan[5] measured fluctuating forces on a stationary circular cylinder over a range of Reynolds number. The corresponding preliminary results for square and rectangular cylinders were presented by Modi and Heine.[6]

Among the numerous papers written on the aspects of fluid mechanics and dynamics of bluff bodies, only a few are concerned with the actual measurements of unsteady pressures. McGregor[7] and Gerrard[8] measured fluctuating forces on a circular cylinder using a condenser microphone system built into the model. Pendergast[9] obtained spanwise pressure correlation results for a stationary cylinder using a modified form of McGregor's apparatus. Keefe[10] carried out fluctuating force measurements with the help of a carefully designed strain-gage transducer that also acted as a test model. Molyneux[11] has also described a low-frequency strain-gage type transducer mounted inside the model to measure pressures on oscillating wings.

Modi and Heine[12] and Ferguson and Parkinson[13] designed pressure transducers, using a piezoelectric crystal and light sensitive resistance, respectively, which were located externally and connected to the pressure taps on the model by a series of polyethylene tubings. The devices exhibited several undesirable features. The former has a marginal sensitivity whereas the latter, though sensitive, was substantially affected by the ambient temperature and humidity.

The available information concerning bluff body interaction with the separated flow of stable vortex street type is not limited to the cylinders of circular cross section. Investigations with square, rectangular, triangular, and hexagonal cylinders, structural H and angle sections, as well as several irregular geometries are reported. But it must be emphasized that the

Presented as Paper 69-745 at the CASI/AIAA Subsonic Aero- and Hydro-Dynamics Meeting, Ottawa, Canada, July 2–3, 1969; submitted August 4, 1969; revision received April 24, 1970. The investigation was supported by the National Research Council and Defense Research Board Grants A-2181 and 9550-38, respectively.

* Professor.

† Graduate Research Assistant; at present, Research Engineer, A. B. Volvo, Göteborg, Sweden.

bulk of the literature is indeed devoted to the circular geometry. This point is well emphasized by the fact that the previous work on elliptical cylinders seems to be limited to rather preliminary unsteady pressure measurements by Heine[14] and the Strouhal number study of Schramm.[15]

The aeroelastic instability of bluff bodies has been under investigation at this University since 1958. The review of the progress made has been reported in two survey papers.[16,17] The investigation described here forms the part of this continuing program.

2 Models and Supporting System

Two elliptic cylindrical models, 27 in. long, were designed to span the wind-tunnel cross section thus approximating the two-dimensional flow condition. The physical parameters are listed in Table 1.

The central bulkhead of each model carried 32 pressure taps, of diameter 0.025 in., equally spaced around the circumference (Fig. 1). The pressure taps were connected to plastic tubes of inside diameter 0.066 in. that were brought out from one end of the cylinder. In the case of the plexiglas model it was thought advisable, because of the thin skin, to ascertain the rigidity of the panel. A simple test of deflection and natural frequency showed the panels to be of adequate stiffness with a maximum deflection of less than 0.0004 in. and natural frequency of 180 cps during operating conditions.

The models were tested in a low-speed, low-turbulence, return type wind tunnel where the air speed can be varied from 4–150 fps, with a turbulence level less than 0.1%. The pressure differential across the contraction section of 7:1 ratio can be measured on a Betz micromanometer with an accuracy of 0.2 mm of water. The rectangular cross section, 36 × 27 in., is provided with 45° corner fillets which vary from 6 × 6 in. to 4.75 × 4.75 in. to compensate partly for the boundary-layer growth. The spatial variation of mean velocity in the test section was found to be less than 0.25%. The tunnel is powered by a 15 hp direct current motor driving a commercial axiflow fan with a Ward-Leonard system of speed control.

3 Instrumentation and Calibration

The measurement of the acoustic level pressure variations caused by shedding vortices was accomplished using the Barocel Modular Pressure Transducing System developed by Datametrics Inc. of Waltham, Mass. Barocel is a high-precision, stable capacitive voltage divider, the variable element of which is a thin prestressed steel diaphragm. Positioned between fixed capacitor plates, the diaphragm deflects proportional to the magnitude of the applied pressure. An a.c. carrier voltage at 10 kc is applied to the stationary capacitor plates. The diaphragm attains a voltage level determined by its relative position between the fixed capacitor plates. With the Barocel appropriately arranged in a bridge circuit, the output voltage is determined by the ratio of capacitance of the diaphragm to each of the stationary electrodes. The carrier voltage is thereby amplitude modulated in accordance with the input pressure. The unit is capable of measuring pressure down to 0.1 μ of mercury.

The Barocel is accurately calibrated for static pressure. However, for the fluctuating pressure signals transmitted

Table 1 Model data

Model	e	a/b, in./in.	Material	Weight, lb	Number of bulkheads	Skin thickness, in.
1	0.6	2.5/2	Aluminum	4.20	7	0.02
2	0.8	2.5/1.5	Plexiglas	1.45	7	0.02

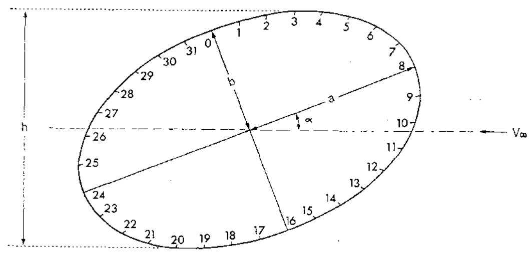

Fig. 1 Numbering system for pressure taps.

through relatively long tubes it was essential to calibrate the unit under simulated operating condition. This required the development of a system where no resonance condition would exist between the transducer with tube and pressure tap on one side and the volume where the calibration signal was generated on the other side. This condition was obtained with sufficient accuracy by using as a pressure source a 5 gal drum with a thin latex diaphragm on one end. The pressure signal was generated by a baffle plate actuating the diaphragm. The plate was driven by a vibration excitor which in turn received its impulse from a function generator. The natural frequency of the drum with diaphragm, baffle and vibration generator was found to be 60 cps.

The natural frequency of the Barocel diaphragm itself is given by the manufacturer to be 2500 cps or higher. Also, the transient response is specified to be less than 2 msec. The Helmholtz resonator frequency of the cavity and the connection on one side of the diaphragm was calculated to be 290 cps. The experimental value obtained by actuating one side of the Barocel with a horn driver was found to be around 210 cps. It was established, through preliminary experiments, that the required frequency range would be from 5 to 35 cps. Considering the lower value of 210 cps for the natural frequency, and a driving frequency of 40 cps, one would get an output within ± 4% of the input for a linear system with damping coefficient somewhere between zero and critical.[18]

Since noticeable attenuation occurred because of the presence of a constriction in the tube all calibrations were performed with pressure tap in the circuit. Moreover, for work in the wind tunnel it was found impossible to use atmospheric pressure as reference. This is because the difference between the static pressure at the tap and the atmospheric pressure was found to be so large as to throw the Barocel off scale at sensitive settings. Moreover, surges in the mean wake condition close to the model affected the pressure field around its surface and gave rise to the same effect. Hence, the final calibration set-up incorporated a damping volume between the pressure ports of the Barocel, thus using the mean static pressure of the tap in question as reference. The effect of amplitude and frequency on output, with the damping bottle in the circuit, is shown in Fig. 2.

The wake survey was carried out using a disc probe constructed by Ferguson[19] and described by Bryer et al.[20] As pointed out by these investigators, the probe is relatively insensitive to pitch (±4°) and yaw (±20°).

It was necessary to introduce a band pass filter in the pressure measuring system to eliminate the undesirable noise. During measurements the filter was calibrated for every change affecting the vortex shedding frequency. Operating the filter at midband frequency and with the high and low cutoff settings separated by a factor of 1.5 gave an attenuation between 0.8 and 0.9. This was found by feeding a sinusoidal signal from the function generator to the rms voltmeter and measuring the difference in output with and without the filter.

Because of considerable, seemingly random, amplitude modulations of the fluctuating pressure it was convenient to present the results as time-average values. Under certain conditions several minutes of averaging was required to get re-

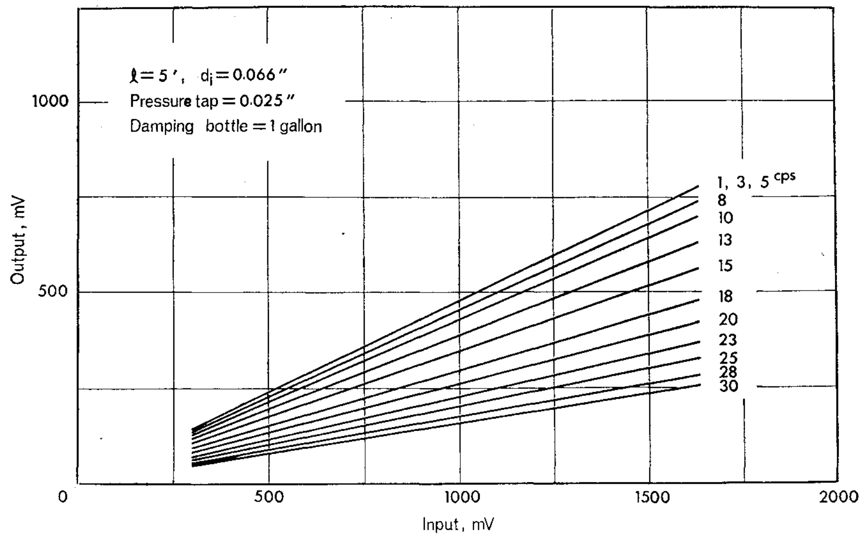

Fig. 2 Calibration plots for Barocel pressure transducer with damping bottle.

producible results. This led to the necessity of using a true rms voltmeter converting the fluctuating pressure signal to an equivalent d.c. signal. An external r-c damping circuit with time constant of 0–60 sec was used to reduce the variations caused by the amplitude modulations. The final steady d.c. level was then measured on the vacuum tube voltmeter.

4 Test Procedures

The diagrammatic lay-out of the apparatus used for fluctuating pressure measurements is given in Fig. 3. During measurements the r-c damping circuit was set to give minimum variation of the voltmeter reading. The fluctuating pressure signal was also displayed on the oscilloscope to determine the maximum amplitude and Strouhal frequency.

The phase between the fluctuating pressures at different taps was obtained by feeding the signals to the Visicorder and measuring the average phase shift over 20 cycles. The effect of any phase change in the instrumentation was nullified by measuring all phase shifts from a permanent reference tap at 90° to the wind direction. The data showed considerable scatter which increased with the distance from the reference tap.

Mean pressure on the model was measured using a Lambrecht manometer. One leg of the manometer was connected to a total head tube in the settling chamber and the other to the pressure tap on the model.

The determination of wake geometry was accomplished using the method described by Heine[14] and Ferguson.[19] The transverse distance between the vortex centrelines was measured by the wake probe connected to the pressure transducer in a manner similar to that shown in Fig. 3. Moving the probe across the wake and plotting the rms value of the signal gave two peaks close to the vortex centrelines. The distance

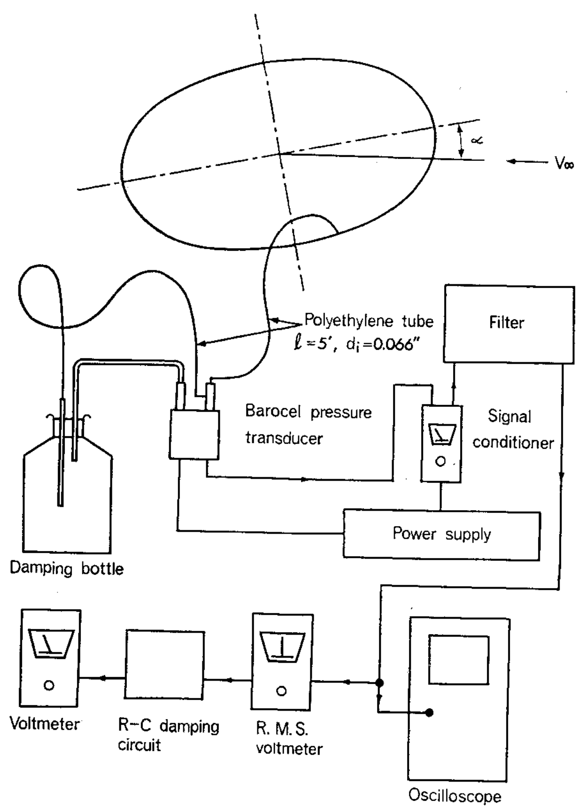

Fig. 3 Schematic representation of the instrumentation used in fluctuating pressure measurement.

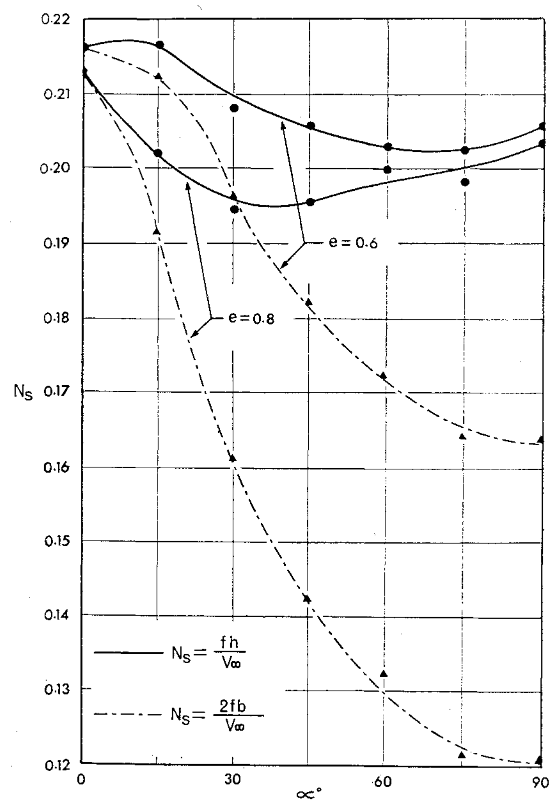

Fig. 4 Variation of Strouhal number with angle of attack.

between the peaks represents, with reasonable accuracy, the lateral spacing between the vortex core lines at that station. The longitudinal spacing between the consecutive vortices was obtained by using a pressure tap as reference and moving the probe downstream on the same side of the model until the signals were 180° out of phase. From this position the probe was moved further downstream so that the signals were in phase. The process was repeated until limited by the travel of the traversing gear. Twice the distance between two successive measurements gave the desired longitudinal spacing between the vortices.

5 Test Results and Discussion

5.1 Strouhal Number

The Strouhal frequency was measured in the Reynolds number range of 2×10^4–10^5 for three different angles of attack, and it was observed to vary linearly with wind speed. The effect of angle of attack on the Strouhal number was also obtained in the same Reynolds number range. These variations based on the minor axis as well as the projected height are shown in Fig. 4.

The Strouhal number based on projected height showed comparatively less dependence on the angle of attack in the Reynolds number range investigated. An observation concerning the Strouhal number variation at low angles of attack is pertinent here. For the thicker ellipse a slow rise in the projected height with a small drop in shedding frequency leads to an almost uniform Strouhal number in this range. On the other hand, for the thinner ellipse the very sharp drop in shedding frequency offsets the relatively greater rise in projected height thus leading to a decrease in Strouhal number. The similar tendency was also observed by Schramm.[15] In all cases except one, Schramm's measurements were limited to 0–45° range due to, as reported by him, "lack of stable vortex street." This is in contrast to the strong and well defined fluctuating signals observed in the results presented here.

A modulation of the vortex shedding frequency was present at all times. It amounted to as much as ±5%, and may be related, to some extent, to the amplitude modulation. The frequency modulation was too small to affect the filter calibration.

5.2 Fluctuating Pressure Distribution

For both ellipses, the effect of varying the Reynolds number in the range 3×10^4–10^5 was investigated for $\alpha = 0, 30°, 60°, 90°$. In each case, to reflect the influence of flow character, the fluctuating pressure measurements were taken at four taps, two in the laminar and the other two in the separated flow regions. The Reynolds number was varied systematically and rms value of the unsteady pressure at a given tap was noted. Average value of the pressure over the Reynolds number range was determined at each tap. The results plotted in Fig. 5 represent the percentage variation about the mean of the pressure coefficient at each of the ports in question.

No significant Reynolds number effect was noticed except for the abrupt increase in the fluctuating pressure coefficient at zero angle of attack and low wind speed. The cause of this phenomenon is not quite clear, but it should be emphasized that it is not associated with any noticeable change in base pressure. This, together, with the Reynolds number at which the behaviour occurred, makes it unlikely to be due to either proximity to the critical Reynolds number or any other change in character of the separation.

The unsteady pressures on the surface of the two elliptic models were recorded for $\alpha = 0, 30°, 60°$, and $90°$. These results are plotted in Fig. 6 together with the mean pressure distribution.

Based on these results the following remarks can be made.

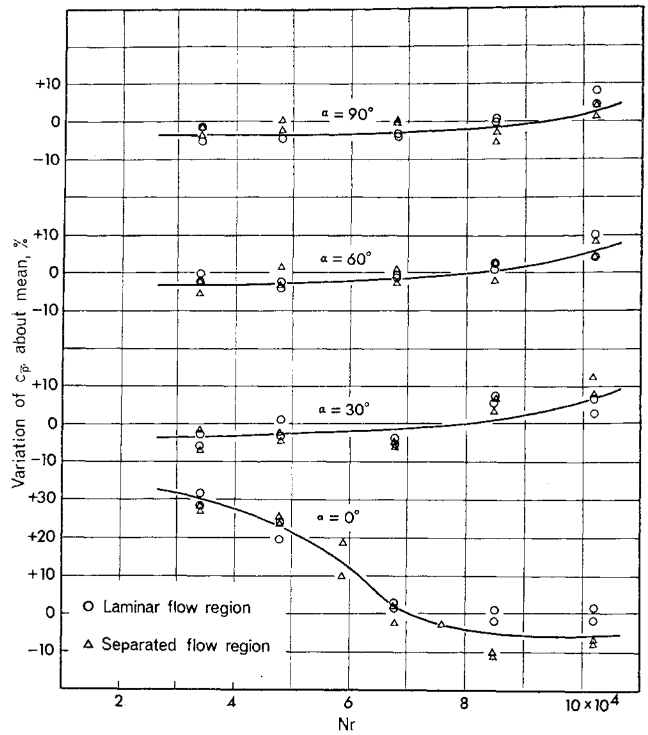

a) $e = 0.6$

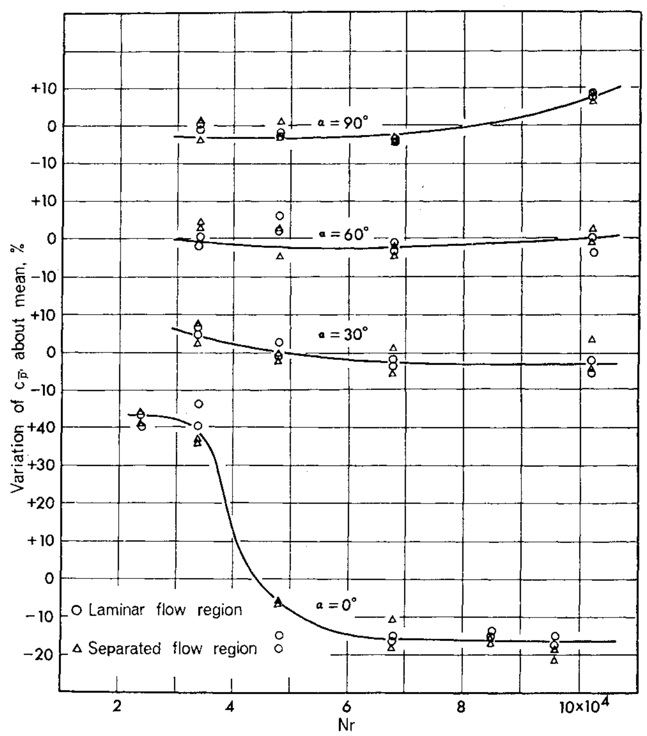

b) $e = 0.8$

Fig. 5 Variation of fluctuating pressure coefficient with Reynolds number.

1) There are two points where the fluctuating pressure tends to vanish. They occupy positions which are approximately 180° apart and represent the "stagnation points." One would expect this due to cancellation of pressures which are 180° out of phase. As shown in Fig. 6 this effect is less complete at the rear of the cylinder, probably due to irregularities in the wake.

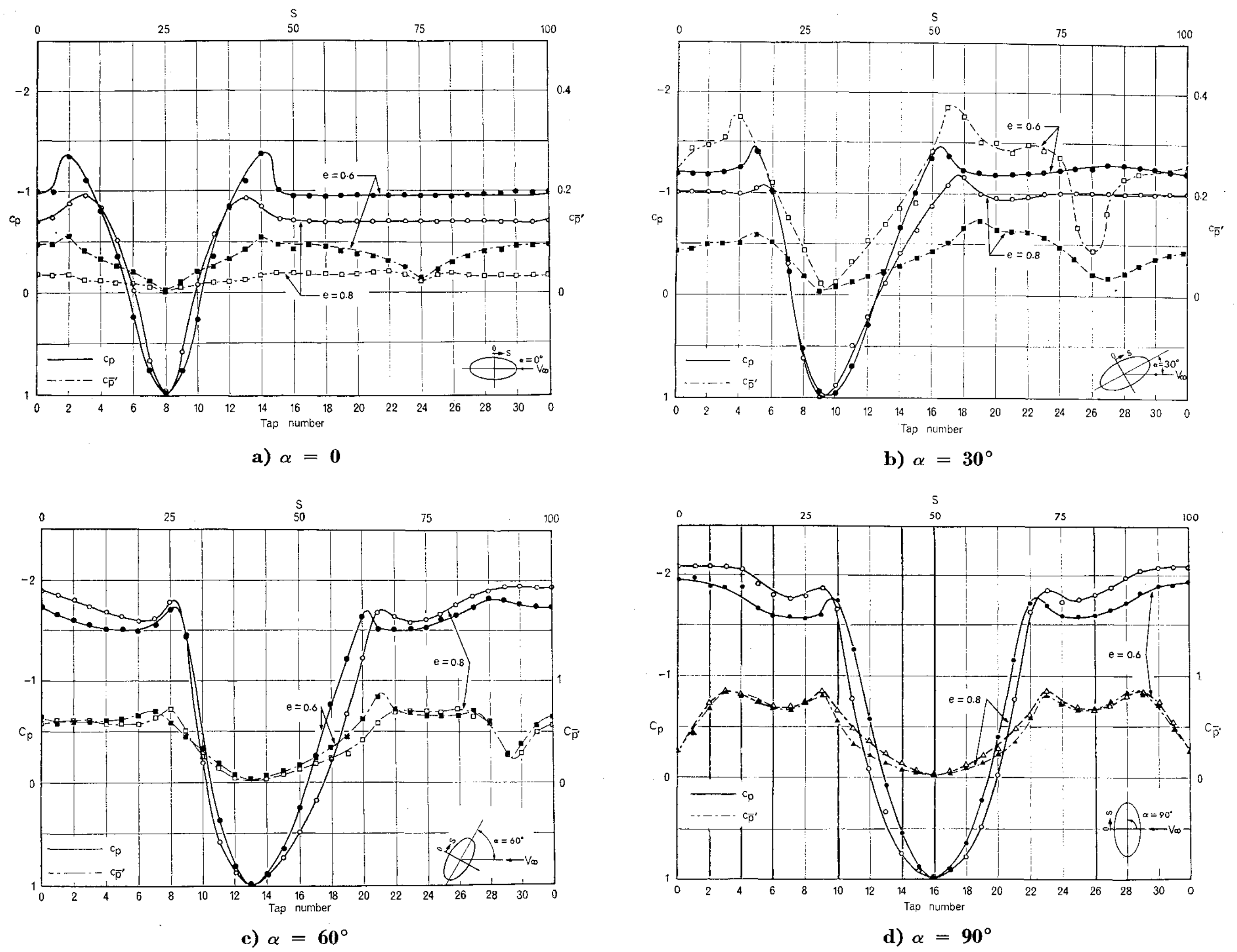

Fig. 6 Distribution of mean and fluctuating pressure coefficients.

2) The fluctuating pressure increases as the mean pressure decreases and, in general, the variations can be represented by curves following a similar trend.

3) The mean base pressure diminishes with increase in angle of attack. The same is true for the unsteady pressure. But, while the mean pressure coefficient approximately doubles in the range $\alpha = 0$–$90°$ the corresponding increase in fluctuating pressure coefficient is as high as 10–20 times.

4) As expected, at zero angle of attack, the fluctuating pressure coefficient for the slender ellipse is considerably less than that for the thicker ellipse, but at 90° they are practically equal.

Variation of the maximum fluctuating pressure coefficient with angle of attack is shown in Fig. 7. To illustrate the amount of amplitude modulation present in the fluctuating pressure signals, the ratio between the maximum and the average amplitude has been plotted in Fig. 8. The results showed considerable scatter, but the increase in maximum/average ratio towards the rear "stagnation point" was quite distinct. There was also a trend towards a reduction of the ratio in the laminar flow region. As stated by several investigators[7,8,14,19] the amplitude modulations were found to be in phase around the models.

5.3 Phase Shift

Gerrard[8] was probably the first one to measure phase relation between the fluctuating pressure signals on a circular cylinder. He used two built-in pressure transducers that could be rotated individually and concluded that the pressures were essentially in phase over one side of the model and 180° out of phase with that on the other side. Any deviation from this was attributed to the spanwise separation between the pressure taps.

The present experiments confirmed the 180° phase difference between pressures on two sides of the model. But contrary to Gerrard's observation it indicated substantial phase shift between the signals from the neighboring pressure taps. The phase measurement was carried out on both elliptical models at $\alpha = 0, 90°$, and the results are plotted in Fig. 9.

It is apparent that for the models at $\alpha = 0$ the signals from upstream and downstream pressure taps are lagging and leading, respectively, with respect to the reference located at the 90° position (tap 16 or 32). On the other hand at $\alpha = 90°$ all signals lag the reference (tap 8 or 24). The phase difference between two pressure signals was found to be as large as 60°.

Table 2 Effect of phase shift on fluctuating lift coefficient

e	$\alpha°$	$C_{\bar{l}'}$	$(C_{\bar{l}'})$ phase	% change in $C_{\bar{l}'}$
0.6	0	0.156	0.152	2.5
	90	1.007	1.001	0.5
0.8	0	0.064	0.060	6.0
	90	0.719	0.710	1.0

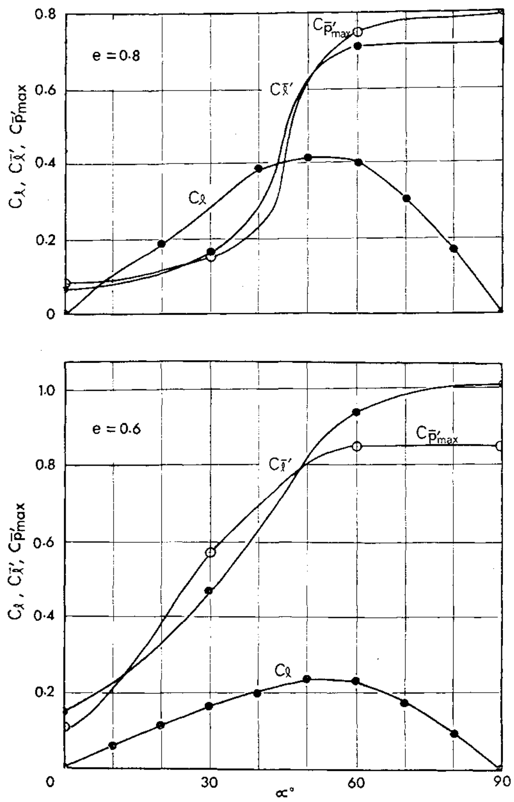

Fig. 7 Variation of lift and maximum fluctuating pressure coefficients with angle of attack.

5.4 Fluctuating Lift

The fluctuating lift coefficients for both ellipses at $\alpha = 0$, 30°, 60°, and 90° were calculated from the pressure data given earlier. The results are plotted in Fig. 7. For either ellipse the maximum fluctuating lift $[(1.0)_{e=0.6}, (0.72)_{e=0.8}]$ was found at 90° while the minimum value occurred at $\alpha = 0$. The fluctuating lift coefficient for a circular cylinder as obtained by McGregor[7] was 0.6.

It may be pointed out that the maximum and minimum values given previously were obtained without taking phase shift into account. With phase angle between the pressure signals the corresponding values are modified as shown in Table 2.

5.5 Wake Geometry

Typical average amplitude signals across the wake are given in Fig. 10a. It was found that after a downstream distance of nearly three major axes the spacings between the vortices remained approximately constant. The wake signals at $\alpha = 0$ became too weak to be recorded at 20–30 in. downstream. On the other hand, more powerful signals at higher angles of attack could be observed down to 45 in. which was the limit for the measuring rig. For $\alpha = 30°$ and 60° the wake was slightly unsymmetrical, the vortex from the rearmost separation point being the stronger. Typical decay of pressure am-

Table 3 Spacing of vortices in fully developed wake, $Nr = 70{,}000$

	$e = 0.6$			$e = 0.8$			$e = 0^a$
α	L, in.	W, in.	W/L	L, in.	W, in.	W/L	W/L
0	16.00	5.0	0.31	10.00	4.3	0.42	0.32
30	19.25	5.2	0.27	16.50	5.1	0.31	
60	21.75	5.7	0.26	20.75	5.7	0.28	
90	22.75	5.8	0.26	22.25	5.9	0.26	

^{a} Ref. 13.

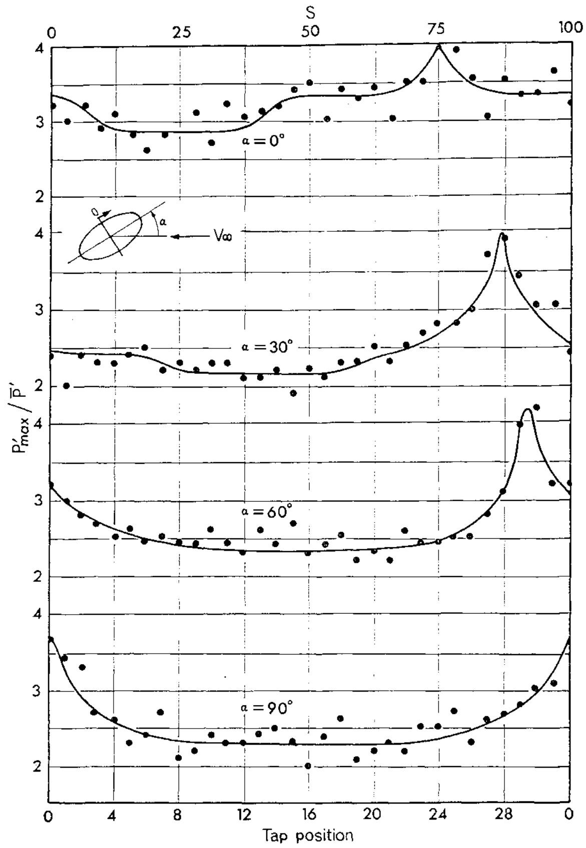

a) $e = 0.6$

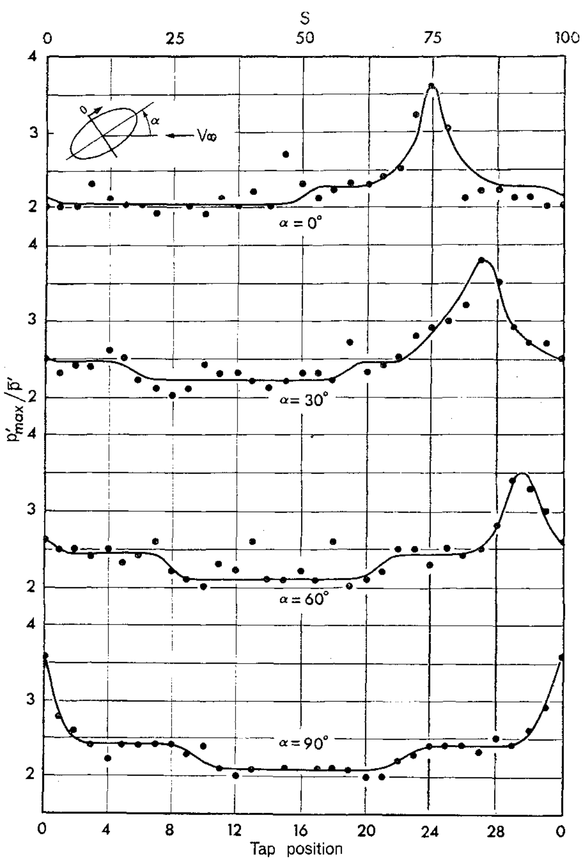

b) $e = 0.8$

Fig. 8 Amplitude modulation of the pressure signals on the surface of the model.

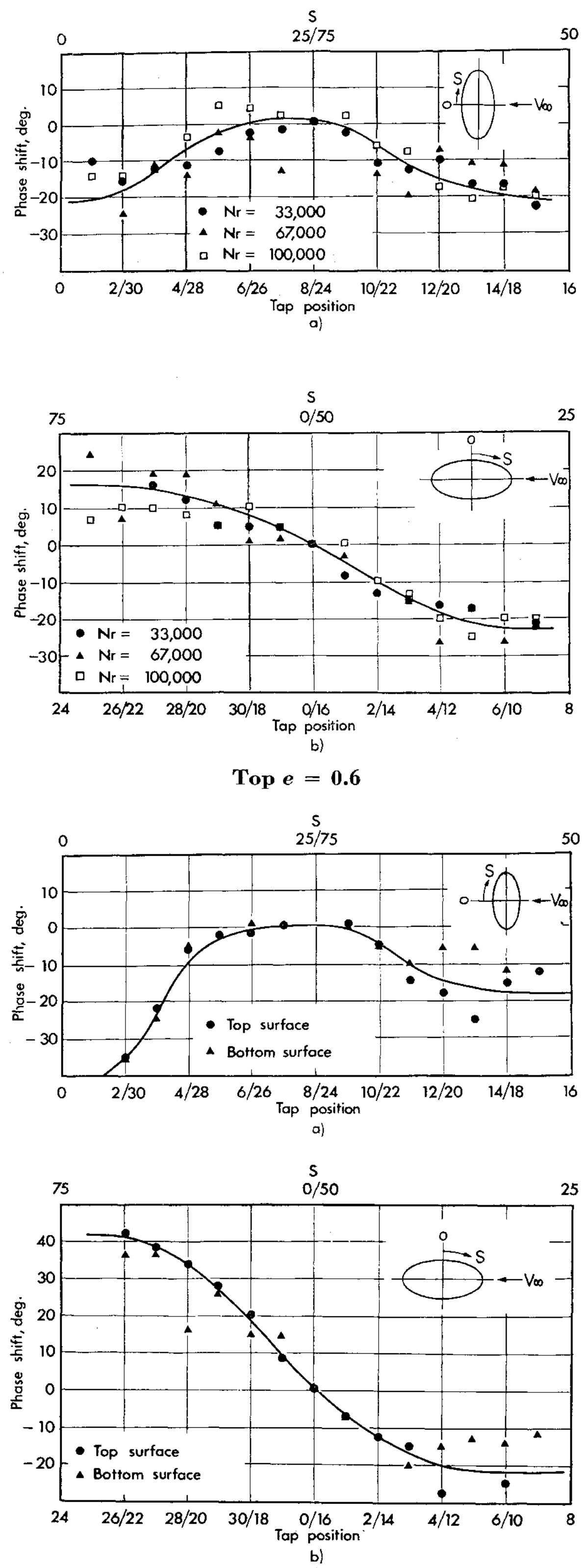

Fig. 9 Phase shift between pressure signals on the surface of the model at Nr = 67,000.

plitude with downstream distance is given in Fig. 10b. Average values for the spacing between vortices are given in Table 3.

Within the range of the Reynolds number investigated no significant change in wake geometry occurred. A remark concerning wind-tunnel wall corrections would be appropriate.

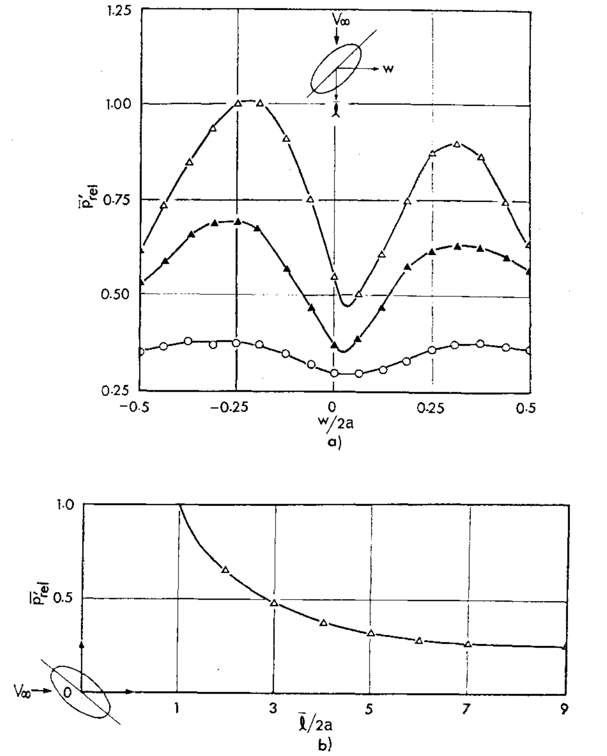

Fig. 10 Representative results of wake measurements: a) typical wake traverse, b) typical plot of pressure decay in wake.

There is some information available[21,22] for approximate prediction of equivalent free flight results from wind tunnel measurements so far as steady flow is concerned. Unfortunately, for fluctuating pressures apparently no reliable method for predicting correction is available, probably because the situation is considerably more complex. In addition to blockage influencing both fluctuating pressure and vortex frequency is a velocity field due to wake vortices. Moreover, the periodic character of the flow may lead to an expression for wall correction which is also periodic in nature.

6 Concluding Remarks

Based on the experimental results the following general remarks can be made concerning unsteady aerodynamics of the elliptic cylinders tested.

1) The Strouhal frequency, which shows slight modulation, increases linearly with wind speed. The variation of Strouhal number with angle of attack is considerably less when based on projected height.

2) The fluctuating pressure coefficients tend to increase with angle of attack. In the range α = 0–90°, $C_{\bar{p}_{max}}$, increased from 0.1 to 0.8 for e = 0.6 and from 0.04 to 0.8 for e = 0.8. Marked dependency on the Reynolds number appears to be limited to zero angle-of-attack condition. The pressure signals are always amplitude modulated and the extent of modulation, as expressed by $p_{max}'/\bar{p}'$ is of the order 2–4.

3) Pressure signals on the surface of the models have considerable phase differences. At times this can be as high as 60°.

4) Similar to the fluctuating pressure coefficients, the lift coefficients are affected by the attitude of the models. The maximum lift coefficients (based on the major axis) were found to be 1.0 and 0.7 for e = 0.6 and 0.8, respectively. The phase shift has only small effect on these values.

5) The ratio of the transverse to the longitudinal spacing between vortices in the wake decreases with increasing angle of attack. This was observed to be true for both ellipses but the reduction was more pronounced for the thinner ellipse.

6) For $\alpha = 0$ the separation points for the boundary layer as indicated by the static pressure distribution occurs at approximately the same angular position ($\approx 75°–80°$) for both ellipses. This appears reasonable compared to the experimentally measured value of $\approx 82°$ for a circular cylinder.[23]

References

[1] Strouhal, V., "Über eine Besondere Art der Tonerregung," *Wiedschrift Annalen der Physik und Chemishe*, Neue Folge, Vol. V, 1878, pp. 216–251.

[2] von Kármán, T., "Flussigkeit und Luftwiderstand," *Physik Zeitschrift*, Vol. 13, 1911, p. 49.

[3] Marris, A. W., "A Review of Vortex Streets, Periodic Wakes, and Induced Vibration Phenomena," *Transactions of the ASME: Journal of Basic Engineering*, Vol. 86, June 1964, pp. 185–196.

[4] Grove, A. S. et al., "An Experimental Investigation of the Steady Flow Past a Circular Cylinder," *Journal of Fluid Mechanics*, Vol. 19, Pt. 1, May 1964, pp. 60–80.

[5] Bishop, R. E. D. and Hassan, A. Y., "The Lift and Drag Forces on a Circular Cylinder in a Flowing Fluid," *Proceedings of the Royal Society of London*, Ser. A, Vol. 277, Jan. 1964, pp. 32–50.

[6] Modi, V. J. and Heine, W., "On the Pressure Fluctuations and Wake Geometry Associated with Several Bluff Bodies," *Proceedings of the 15th Japan National Congress of Applied Mechanics*, Japan Society of Mechanical Engineers, 1966, pp. 7–18.

[7] McGregor, D. M., "An Experimental Investigation of the Oscillating Pressures on a Circular Cylinder in a Fluid Stream," TN 14, June 1957, Univ. of Toronto Institute of Aerophysics, Toronto, Ont.

[8] Gerrard, J. H., "An Experimental Investigation of the Oscillating Pressures on a Circular Cylinder Shedding Turbulent Vortices," *Journal of Fluid Mechanics*, Vol. 11, Pt. 2, Sept. 1961, pp. 244–256.

[9] Prendergast, V., "Measurement of Two-Point Correlations of the Surface Pressure on a Circular Cylinder," TN 23, July 1958, Univ. of Toronto Institute of Aerophysics, Toronto, Ont.

[10] Keefe, R. T., "An Investigation of the Fluctuating Forces Acting on a Stationary Circular Cylinder in a Subsonic Stream, and of the Associated Sound Field," Rept. 76, Sept.1961, Univ. of Toronto Institute of Aerophysics, Toronto, Ont.

[11] Molineux, W. G., "Measurement of the Aerodynamic Forces on Oscillating Airfoils," Rept. 35, April 1956, Advisory Group for Aeronautical Research and Development, NATO, Paris.

[12] Modi, V. J. and Heine, W., "A Transducer for the Study of Wake Geometry," *Journal of Scientific Instruments*, Vol. 42, July 1965, pp. 497–498.

[13] Ferguson, N. and Parkinson, G. V., "Surface and Wake Flow Phenomena of the Vortex-Excited Oscillation of a Circular Cylinder," *Transactions of the ASME: Journal of Engineering for Industry*, Vol. 89, 1967, pp. 831–838.

[14] Heine, W., "On the Experimental Investigation of Vortex Excited Pressure Fluctuations," M.Sc. thesis, Aug. 1964, Univ. of British Columbia, Vancouver, B. C.

[15] Schramm W., "Wirbelfrequenzmessungen an umstromten Bauteilen," *Ifl-Mitteilungen*, Vol. 5, No. 8, Aug. 1966, pp. 308–318.

[16] Parkinson, G. V., "Aeroelastic Galloping in One Degree of Freedom," *Proceedings of the First International Conference on Wind Effects on Buildings and Structures*, National Physical Lab., London, Vol. II, 1965, pp. 581–609.

[17] Parkinson, G. V. and Modi, V. J., "Recent Research on Wind Effects on Bluff Two-Dimensional Bodies," *International Research Seminar: Wind Effects on Buildings and Structures*, National Research Council, Ottawa, 1967, pp. 485–513.

[18] Morse, P. M., *Vibration and Sound*, 2nd ed., McGraw-Hill, New York, 1948, pp. 27–42.

[19] Ferguson, N., "The Measurement of Wake and Surface Effects in the Subcritical Flow Past a Circular Cylinder at Rest and in Vortex Excited Oscillations," M.Sc. thesis, Sept. 1965, Univ. of British Columbia, Vancouver, B. C.

[20] Bryer, D. W., Walshe, D. E., and Garner, H. C., "Pressure Probes Selected for Three-Dimensional Flow Measurement," R and M 3037, 1958, Aeronautical Research Committee, England.

[21] Whitbread, R. E., "Model Simulation of Wind Effects on Structures," *Proceedings of the First International Conference on Wind Effects on Buildings and Structures*, National Physical Lab., London, Vol. 2, 1965, pp. 581–610.

[22] Pankhurst, R. C. and Holder, D. W., *Wind-Tunnel Technique*, 1st ed., Pitman and Sons, London, 1952, Chap. 8.

[23] Schlichting, H., "*Boundary-Layer Theory*," 1st ed., McGraw-Hill, New York, 1968, pp. 21, 202–206.